

We are IntechOpen, the world's leading publisher of Open Access books Built by scientists, for scientists

6,900

Open access books available

185,000

International authors and editors

200M

Downloads

Our authors are among the

154

Countries delivered to

TOP 1%

most cited scientists

12.2%

Contributors from top 500 universities



WEB OF SCIENCE™

Selection of our books indexed in the Book Citation Index
in Web of Science™ Core Collection (BKCI)

Interested in publishing with us?
Contact book.department@intechopen.com

Numbers displayed above are based on latest data collected.
For more information visit www.intechopen.com



Nonlinear Friction Model for Passive Suspension System Identification and Effectiveness

Ali I. H. Al-Zughaibi

Abstract

To achieve a high level of performance, frictional effects have to be addressed by considering an accurate friction model, such that the resulting model faithfully simulates all observed types of friction behaviour. A nonlinear friction model is developed based on observed measurement results and dynamic system analysis. The model includes a stiction effect, a linear term (viscous friction), a nonlinear term (Coulomb friction) and an extra component at low velocities (Stribeck effect). During acceleration, the magnitude of the frictional force at just beyond zero velocity decreases due to the Stribeck effect, which means the influence of friction reduces from direct contact with bearings and body into the mixed lubrication mode at low velocity. This could be due to lubricant film behaviour. In respect of acceleration and deceleration when the direction changes for the mass body, friction almost depends on this direction, while the static frictional force exhibits springlike characteristics. However, friction is not determined by current velocity alone, it also depends on the history of the relative wheel and body velocities and movements, which are responsible for friction hysteresis behaviour.

Keywords: nonlinear friction model, stiction region, Stribeck effect, viscous friction, passive suspension system model

1. Introduction

Friction occurs almost everywhere. Many things, including human acts, depend on it. It is usually present in machines. Usually, friction is not required, so a great deal is done to reduce it by design or by control. Friction is often quantified by a coefficient of friction (μ), expressing the ratio of the friction force to the applied load [1].

The spearheading work of Amontons, Coulomb and Euler, who attempted to clarify the friction phenomenon regarding the mechanics of relative movement of rough surfaces in contact with one another, is mentioned by [2]. From that point forward, only sporadic consideration has been paid to the vital question of friction as a dynamic process that changes on contact. Instead, the most significant proportion of the investigation has concentrated on describing and evaluating complex mechanisms, such as adhesion and deformation that contribute to development of frictional resistance, while frequently ignoring the dynamic aspects of the issue. Consequently, despite those mechanisms being relatively well researched, characterised and understood, no efficient and comprehensive model has emerged

for the evolution of the friction force as a function of the states of the system, namely, time, displacement and velocity. The requirement for such a model is now becoming more urgent, since the consideration of the friction force dynamics proves essential to understanding and control of systems, including rubbing elements, from machines to earthquakes. Therefore, if it were possible to qualify and quantify this friction force dynamic, it would be a relatively simple step to treat the dynamics of a whole system comprising friction; thus, our results are consistent with their findings.

Friction is a very complicated phenomenon arising from the contact of surfaces. Experiments indicate a functional dependence upon a large variety of parameters, including sliding speed, acceleration, critical sliding distance, normal load, surface preparation and, of course, material combination. In many engineering applications, the success of models in predicting experimental results remains strongly sensitive to the friction model.

A fundamental, unresolved question in system simulation remains: what is the most appropriate way to include friction in an analytical or numerical model and what are the implications of the chosen friction model?

From a control point of view, control strategies that attempt to compensate for the effects of friction, without resorting to high gain control loops, inherently require a suitable friction model to predict and compensate for the friction. Even though no exact formula for the friction force is available, friction is commonly described in an empirical model. Nevertheless, for precision/accuracy requirement, a good friction model is also necessary to analyse stability, predict limit cycles, find controller gains, perform simulations, etc. Most existing model-based friction compensation schemes use classical friction models, such as Coulomb and viscous friction. In applications with high-precision positioning, the results are not always satisfactory. Friction is a natural phenomenon that is quite difficult to model and is not yet completely understood [3].

From a friction-type point of view, in fluid- or grease-lubricated mechanisms, friction decreases as the velocity increases away from zero. In general terms, this effect is understood. It is due to the transition from boundary lubrication to fluid lubrication. In boundary lubrication, extremely thin, perhaps monomolecular, layers of boundary lubricants that adhere to the metal surfaces separate metal parts. These lubricant additives are chosen to have low shear strength, so as to reduce friction, proper bonding and a variety of other properties such as stability, corrosion resistance or solubility in the bulk lubricant. Boundary lubricants are standard in greases and oils specified for precision machine applications. With the exception of when lubricants and the friction properties of boundary lubricants are a secondary consideration [4], therefore, this study considers transition friction.

This study found that friction helps to remove a vibration, or oscillation, from mass body displacement as the damping contributes in the test rig. That was unexpected because it always caused the system to deteriorate and friction to be incorporated with the primary target of suspension system performance. Therefore, it is vital to consider friction in this study, and this novel contribution takes into account the friction with the test rig and implements a $\frac{1}{4}$ -car suspension model [5]. In addition, the author hopes to contribute towards a reconsideration of friction with conventional car suspension models.

2. Why considering friction within this study?

In the test rig, a $\frac{1}{4}$ -car, to achieve the primary target of this test rig and the design requirements, the designer had to force the mass body to move in vertical

lines. Therefore, a 240 kg mass plate, used to represent a 1/4-car body, is organised to move vertically via two linear bearings. Two rails, THK type HSR 35CA, 1000 mm long and parallel to each other, are used with each linear bearing. A double wish-bone suspension linkage was chosen because it preserves the geometry of a wheel in an upright position independent of the suspension type used. The wheel hub is connected to the chassis, which is attached to the car body. The test rig passive suspension photograph is shown in **Figure 1**, while the schematic diagram is shown here in **Figure 2**.

Surawattanawan [6] conducted a simulation and experimental study for the same test rig without consideration of the real position for the spring and viscous damper (S and VD); as a result, the friction effects were ignored. However, in the author's opinion, the real inclined position of S and VD should be considered. Accordingly, the test rig design and the input type help to generate a normal force at the body bearings and a vertical force relative to body movement, as will be demonstrated by the free body diagram of test rig later. This force is responsible for generating Coulomb friction at body lubricant bearings. In addition, the mass body has been slipped on lubricant bearings; this will undoubtedly generate viscous friction. Therefore, it is essential to consider these frictions in the current study, qualified by the critical effects of friction in any system, as well as their effects on results.

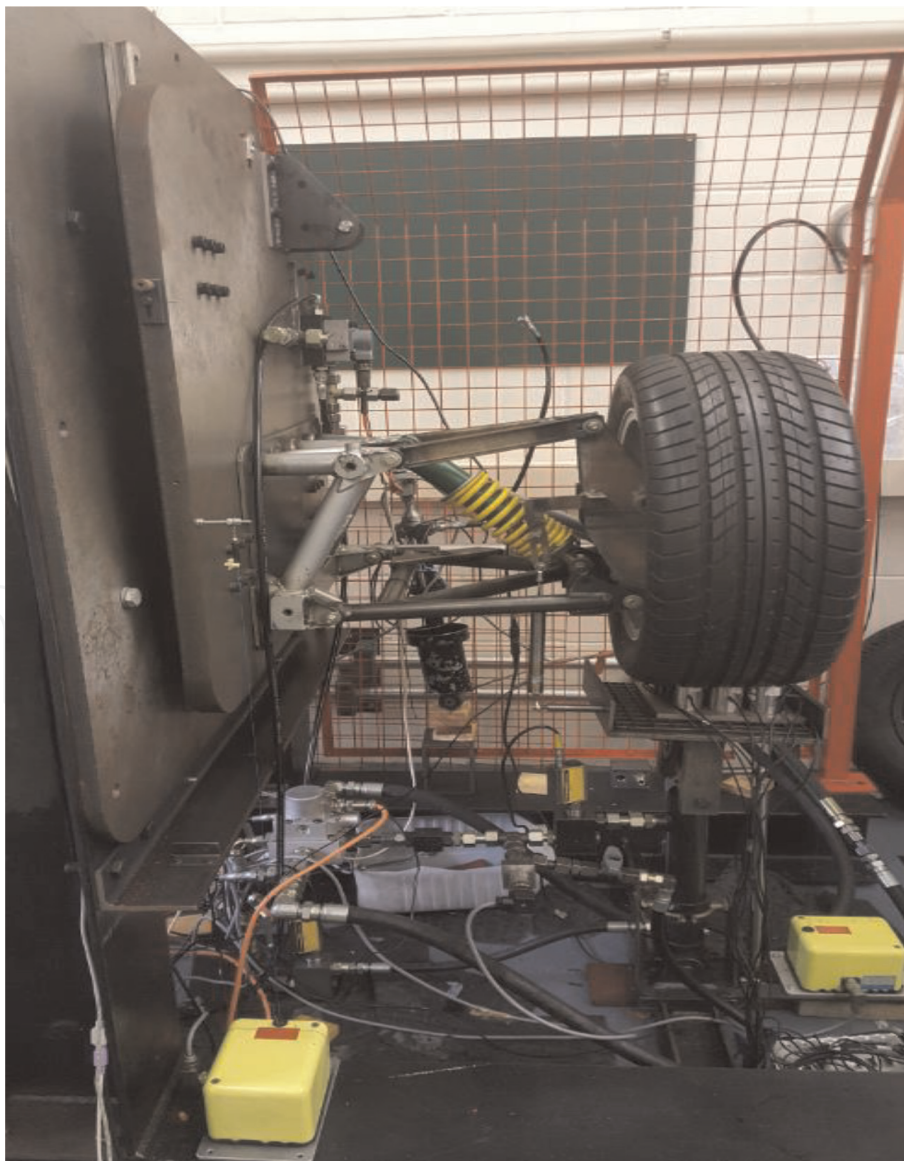


Figure 1.
Photograph of the passive test rig.

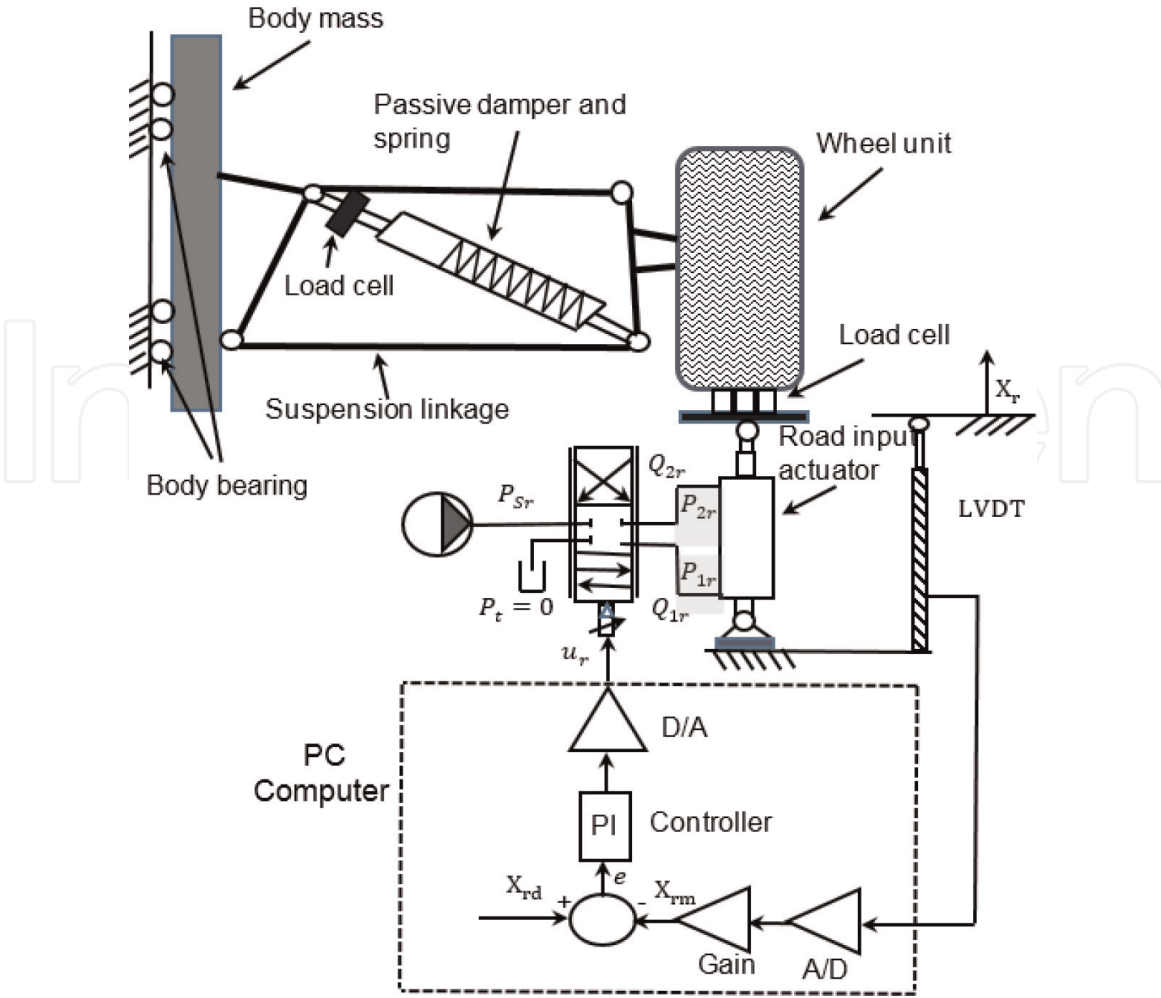


Figure 2.
Schematic diagram of the test rig.

3. Mathematical model of passive suspension system

Vehicle suspensions are designed to minimise car body acceleration \ddot{X}_b , within the limitation of the suspension displacement $X_w - X_b$ and tyre deflection $X_r - X_w$. Hence, the vehicle response variables that need to be examined are:

1. Car body acceleration, \ddot{X}_b
2. Suspension displacement, $X_w - X_b$
3. Tyre deflection, $X_r - X_w$

Using Newton's second law, the equation of motion for the mass body passive system of 1/4-car model is:

$$M_b \cdot \ddot{X}_b = [k_s(X_w - X_b) + b_d(\dot{X}_w - \dot{X}_b)] \quad (1)$$

while the dynamic equation of motion for the mass wheel is:

$$M_w \cdot \ddot{X}_w = -[k_s(X_w - X_b) + b_d(\dot{X}_w - \dot{X}_b)] + k_t(X_r - X_w) + b_t(\dot{X}_r - \dot{X}_w) \quad (2)$$

The constant parameters taken from the test rig are as follows:

Car body mass, $M_b = 240$ kg.
Wheel unit mass, $M_w = 40$ kg.
Tyre stiffness, $k_t = 920000$ N/m.
Tyre damping rate, $b_t = 3886$ N/ms⁻¹
Suspension stiffness, $k_s = 28900$ N/m
Suspension damping, $b_d = 260$ N/ms⁻¹

Following completion of the passive suspension experimental work, an attempt to model these experimental tests is by developing a passive suspension model. The simulation was achieved through developing code in C++. An issue arose in that a considerable difference was found between the body displacement observed in experiments and in the simulation results. From this aspect, the idea of considering friction force emerged. There were two clear indicators from observation measurements, which helped to quantify the friction effects; these are discussed in the following sections.

4. The dynamic indicator

From the simulation results, it was found there are definite fluctuations in body displacement, as generally expected from a quarter-car suspension model, regarding our experience and references. Watton [7] mentioned in his book *Modelling, Monitoring and Diagnostic Techniques for Fluid Power Systems* on pages 182–186, regarding the same test rig, there was an oscillation at the car body in both experimental and simulation results, as shown in **Figure 3**.

It is clearly seen that the body displacement oscillates in the current simulation results, without implementing friction forces, as shown in **Figure 4**. There were differences in the periods of oscillation between **Figures 3** and **4**. This is relative to the different models and parameters used.

There were no such fluctuations in the experimental results, as shown, for example, in **Figure 5**.

Figures 4 and **5** display the desired input, without filter, for the road and the responses of the wheel and body for the present simulation and experimental results, respectively. From these figures, it is clearly seen that the wheel displacement follows the road displacement in both experiment and simulation results, while the body travel follows the wheel with a pure delay, which will be shown in

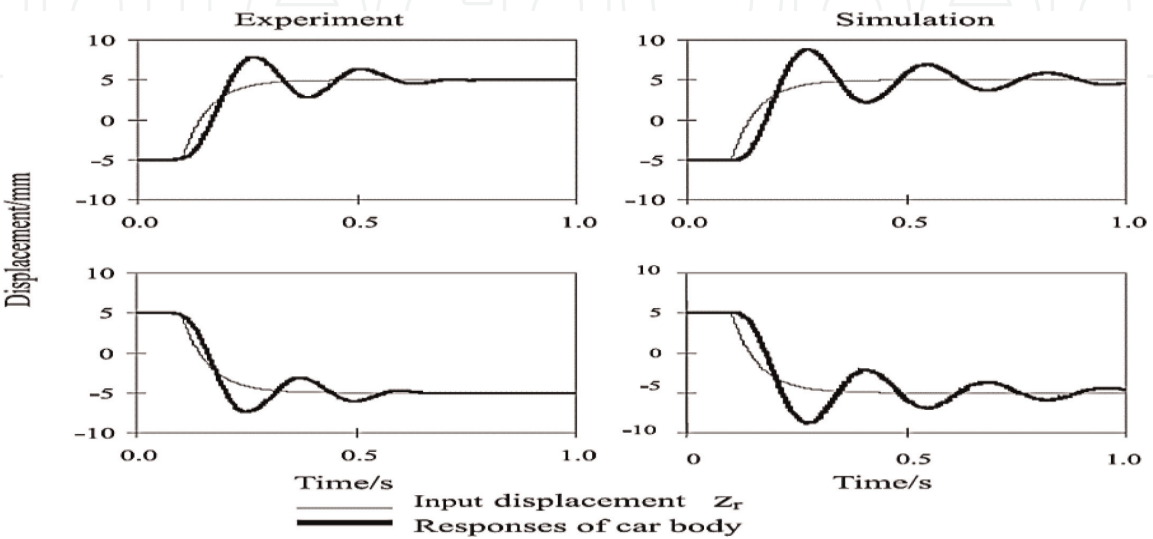
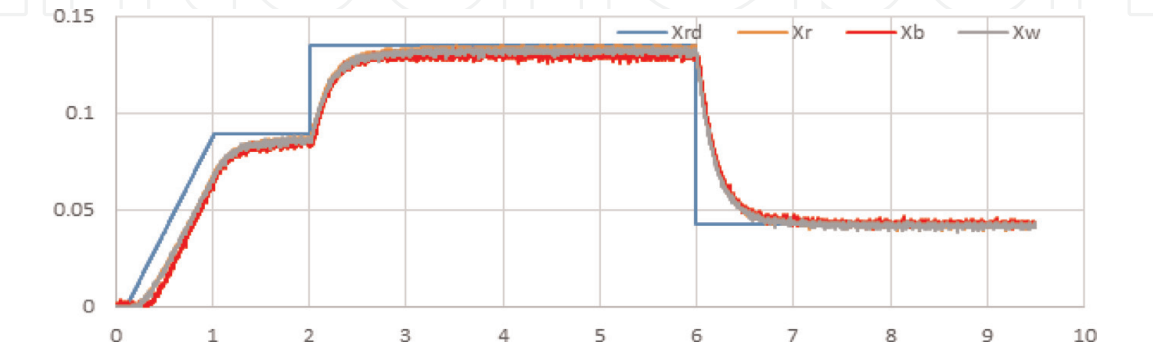
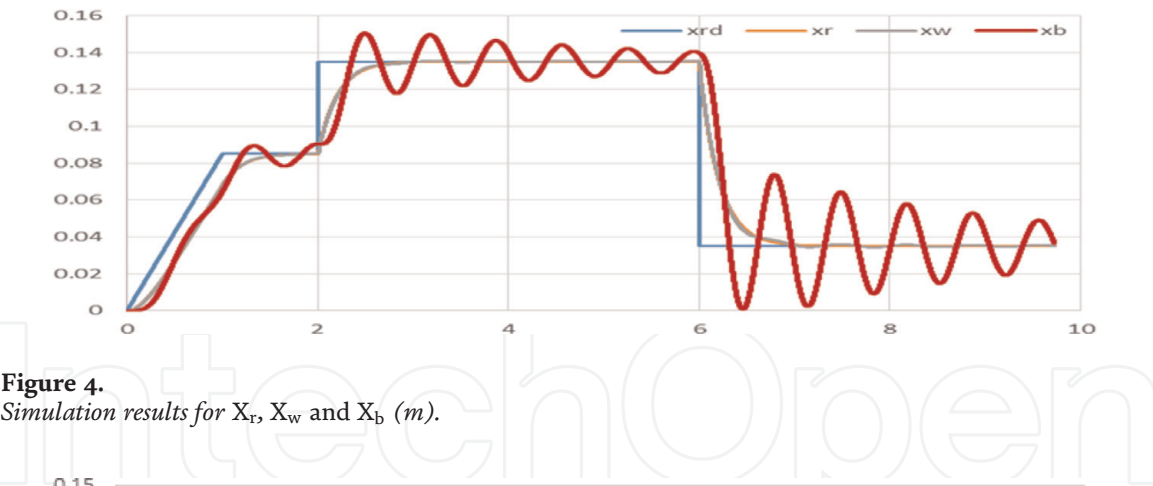


Figure 3.
Typical 1 DOF test result [7].



more detail in Section 5, and fluctuates in the simulation results. The author named this disparity ‘a dynamic friction indicator’. This name was not unique, having been used by several authors before. From this point of view, it could be said that for the experimental work, the friction forces at body lubricant bearings are responsible for eliminating the oscillation from the body travels.

5. The static indicator

In demonstrating the measured body and wheel movements, a delay is illustrated between them when the wheel rises up or falls; the body similarly travels after pure delay. The early and later stages of the wheel rise and fall, respectively; the results to system input and the body delay are shown in **Figure 6**.

For more convenience, the experimental data of the relative travel between the wheel and body ($X_w - X_b$) was used. These are available from test rig from linear variable differential transformer (LVDT) sensors, and the result is shown in **Figure 7**. The evident noise is attributed to sensor and experimental characteristics. From this figure, it is clearly seen that there is zero difference between X_w and X_b at the start of the test or for a short period, approximately 0.3 s. This is believed to be due to data acquisition delays. The differences gradually increase; while the wheel starts to move up, the differences between X_w and X_b steadily increase until reaching the maximum. During this period the body sticks without movement ($X_b = 0.0$); when the resulting force overcomes the static friction, the body will start to move. The relative travel difference between them slowly reduces, approximately 0.5–1.5 s, until reaching zero or near zero at steady state (SS), after 1.5 s.

This observation, which the author named ‘static friction indicator’, leads to an investigation of the body stiction. It was found that this could be regarded as the effect of static friction force.

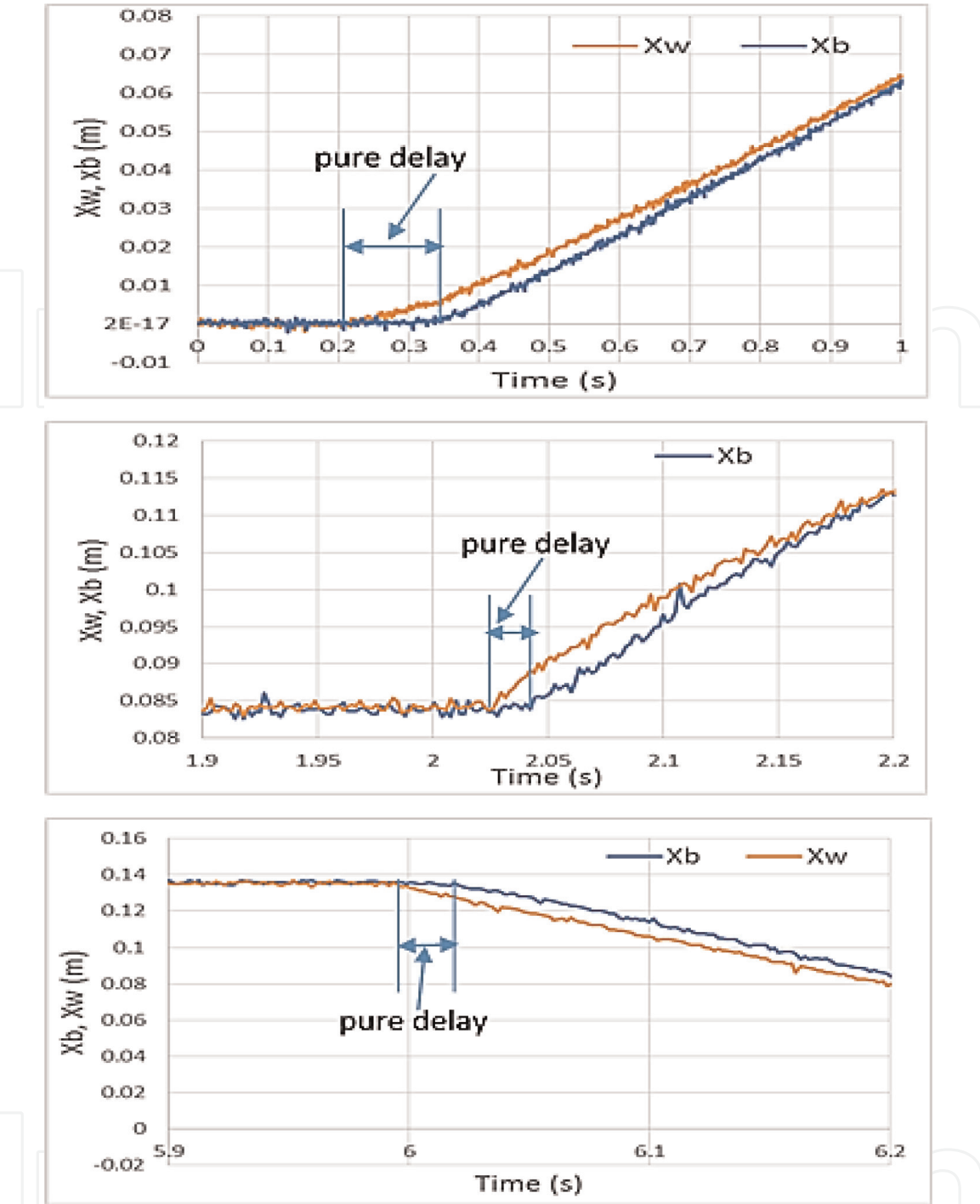


Figure 6.
Measurements of pure delay of X_b from X_w at three positions.

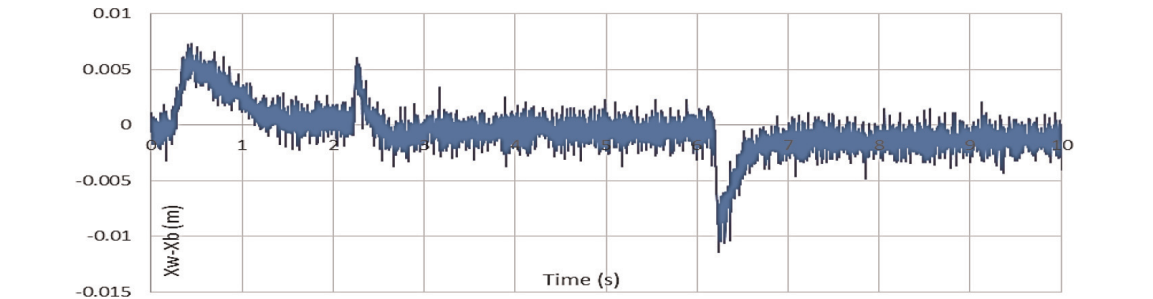


Figure 7.
Experimental results of difference displacements between X_w and X_b .

To include knowledge about friction in the simulation model, consideration of conventional friction was pursued, drawing upon published information. The following section reviews the approach.

6. Conventional friction model

The traditional friction model considered the construction of a more comprehensive friction prediction model that accounts for the various aspects of this particular phenomenon so that mechanical systems with friction can be more accurately identified and, consequently, better controlled. Most of the existing model-based friction compensation schemes use classical friction models, such as Coulomb and viscous friction. In applications with high-precision positioning and with little velocity tracking, the results are not always satisfactory. A better description of the friction phenomena for small speeds, especially when crossing zero velocity, is necessary. Friction is a natural phenomenon that is quite difficult to model and is usually modelled as a discontinuous static map between velocity and friction torque that depends on the velocity's sign. Typical examples are different combinations of Coulomb friction, viscous friction and Stribeck effect, as mentioned in [3, 8, 9]. However, there are several exciting properties observed in systems with friction that cannot be explained by static models. This is necessarily due to the fact that friction does not have an instantaneous response to a change in velocity, i.e. it has internal dynamics. Examples of these dynamic properties [3, 10] are:

- Stick-slip motion, which consists of limit cycle oscillation at low velocities, caused by the fact that friction is more significant at rest than during motion
- Presiding displacement which shows that friction behaves like a spring when the applied force is less than the static friction breakaway force
- Frictional lag which means that there is some hysteresis in the relationship between friction and velocity

The general description of friction is a kind of relation between velocity and friction force, depending on the velocity situations, described in several types of research. For example, Tustin's model consists of Coulomb and viscous friction [11]. The inclusion of the Stribeck effect, with one or more breakpoints, gives a better approximation at low velocities, as shown in **Figure 8**.

Now, in order to start establishing the real bearing friction model, it should involve the dynamic analysis of the test rig as follows:

6.1 How to account for the vertical force

The following explains in detail the main features of the friction model and will begin with how to account for the vertical force that is responsible for generating Coulomb friction by drawing a free body diagram of the test rig.

6.1.1 Free body diagram of the test rig

Figure 9 shows the free body diagram of the test rig; the friction force acts as an internal force in the tangential direction of the contacting surfaces. This force obeys a constitutive equation, such as Coulomb's law, and acts in a direction opposite to the relative velocity. Therefore, the inclination position of S and VD and the system

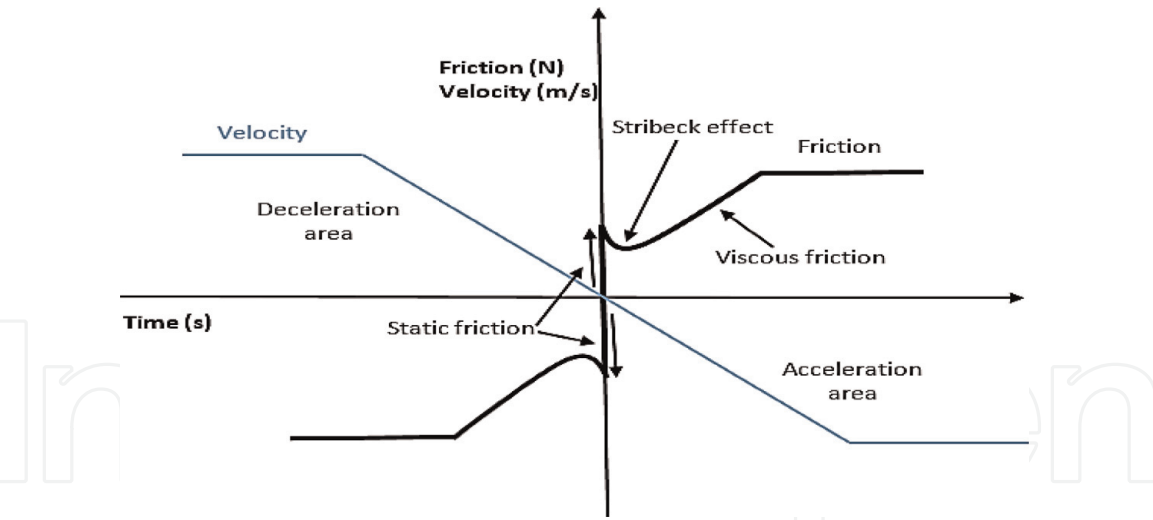


Figure 8.
 Conventional friction model [11].

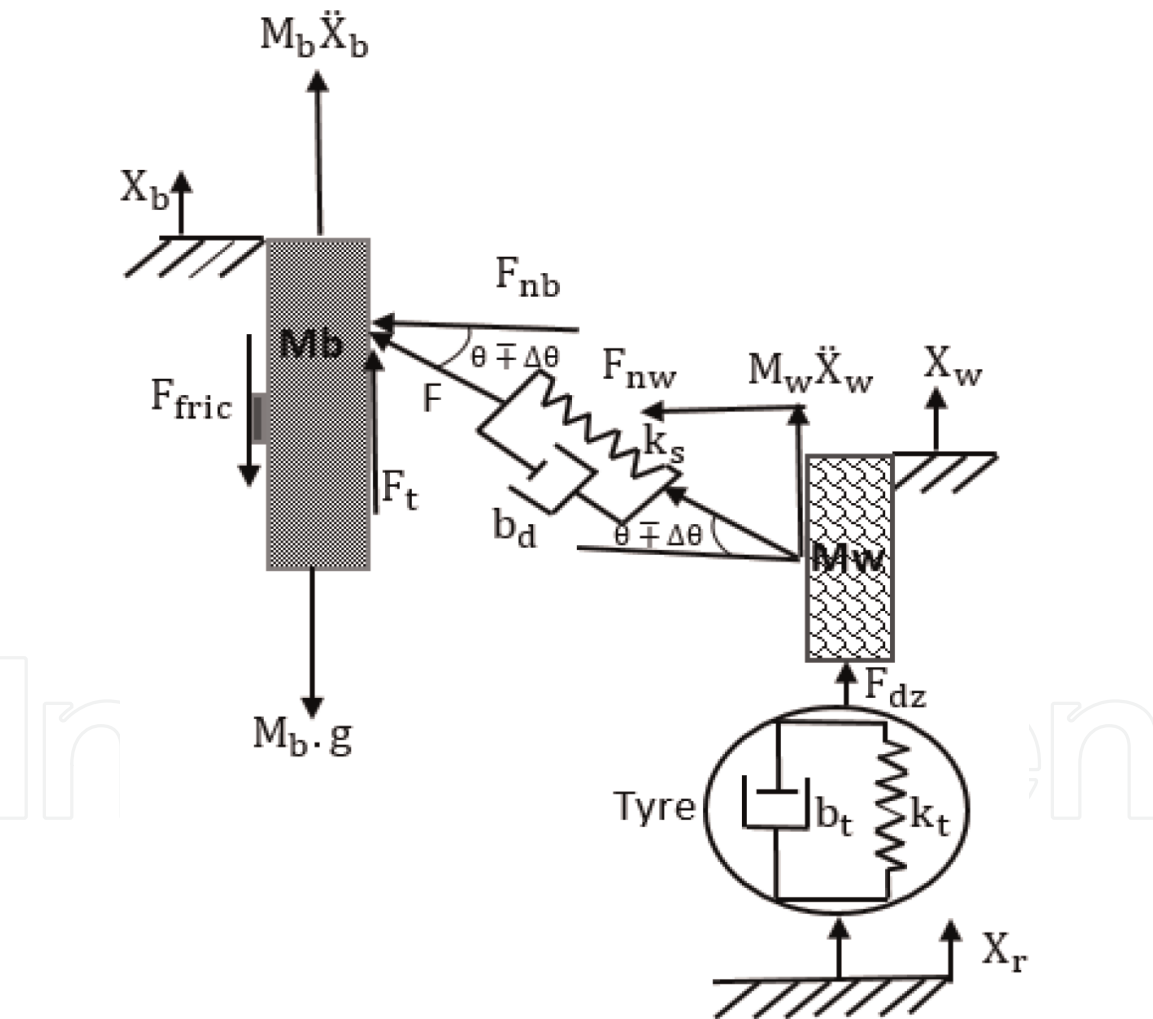


Figure 9.
 Free body diagram of the test rig.

type inputs help to generate the kinematic bearings body friction relative to this normal force component. From **Figure 9**, the following analysis should be conducted to account for this friction force:

$$F = k_s(X_w - X_b) + b_d(\dot{X}_w - \dot{X}_b) / \sin(\theta \mp \Delta\theta) \tag{3}$$

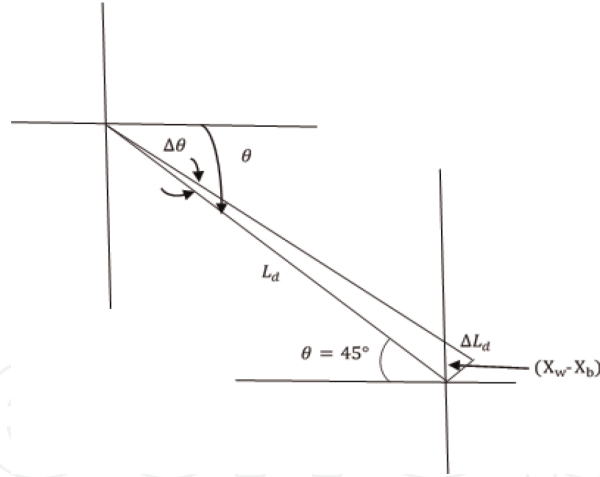


Figure 10.
Engineering geometry of passive units.

$$F_{nb} = F \cos(\theta \mp \Delta\theta) \quad (4)$$

$$F_{nb} = k_s(X_w - X_b) + b_d(\dot{X}_w - \dot{X}_b) / \tan(\theta \mp \Delta\theta) \quad (5)$$

$$F_{fricC} = \mu F_{nb} \quad (6)$$

where F_{fricC} is Coulomb friction, μ is the friction coefficient, F_{nb} is the body normal force component and F is the spring and damping forces.

6.1.2 Dynamic linkage angle expression

The construction linkage angle is dynamically changed by $\mp \Delta\theta$.

From engineering geometry of passive units, as shown in **Figure 10**, it can be found that

$$\frac{L_d - \Delta L_d}{\sin(90 - \theta)} = \frac{X_w - X_b}{\sin(\Delta\theta)}, \theta = 45^\circ \quad (7)$$

$$\sin(\theta) = \frac{\Delta L_d}{X_w - X_b} \quad (8)$$

$\Delta L_d = (X_w - X_b) \sin(\theta)$, where ΔL_d is the dynamic change in S and VD length. Then,

$$\frac{L_d - (X_w - X_b) \sin(\theta)}{\sin(\theta)} = \frac{X_w - X_b}{\sin(\Delta\theta)} \quad (9)$$

$$\sin \Delta\theta = \frac{(X_w - X_b) \sin(\theta)}{L_d - (X_w - X_b) \sin(\theta)} \quad (10)$$

$$\Delta\theta = \sin^{-1} \left[\frac{(X_w - X_b) \sin(\theta)}{L_d - (X_w - X_b) \sin(\theta)} \right] \quad (11)$$

7. Nonlinear friction model

To achieve a high level of performance, frictional effects have to be addressed by considering an accurate friction model, such that the resulting model faithfully simulates all observed types of friction behaviour.

A nonlinear friction model is developed based on observed measurement results and dynamic system analysis. The model includes a stiction effect, a linear term (viscous friction), a nonlinear term (Coulomb friction) and an extra component at low velocities (Stribeck effect). During acceleration, the magnitude of the frictional force at just beyond zero velocity decreases due to the Stribeck effect, which means the influence of friction reduces from direct contact with bearings and body into the mixed lubrication mode at low velocity. This could be due to lubricant film behaviour.

In respect of acceleration and deceleration when the direction changes for the mass body, friction almost depends on this direction, while the static frictional force exhibits springlike characteristics. However, friction is not determined by current velocity alone, it also depends on the history of the relative wheel and body velocities and movements, which are responsible for friction hysteresis behaviour.

This model, which has now become well established, has provided a more satisfactory explanation of observed dynamic fluctuations of body mass. It will be attempted to heuristically 'fit' a dynamic model to experimentally observed results. The resulting model is not only reasonably valid for the $\frac{1}{4}$ -car test rig behaviour but is also reasonably suitable for most general friction lubricant cases.

The model simulates the symmetric hysteresis loops observed in the bearings' body undergoing small amplitude ramp and step forcing inputs. As might be expected, they are capable of reproducing the more sophisticated pre-sliding behaviour in particular hysteresis. The influence of hysteresis phenomena on the dynamic response of machine elements with moving parts is not yet thoroughly examined in the literature. In other fields of engineering, where hysteretic phenomena manifest themselves, more research has been conducted. In Ref. [12], for example, adaptive modelling techniques were proposed for dynamic systems with hysteretic elements. The methods are general, but no insight into the influence of the hysteresis on the dynamics is given. Furthermore, no experimental verification is provided. Altpeter [13] made a simplified analysis of the dynamic behaviour of the moving parts of a machine tool where hysteretic friction was present.

In this study, the friction model, despite its simplicity, can simulate all experimentally observed properties and facets of low-velocity friction force dynamics. Because of the test rig schematic and the system input signal, with historic travel, there are three circumstances depending on whether the body velocity is accelerating or decelerating. Firstly, the velocity values start from zero and just after velocity reversals, reach the highest and are restored to zero, or close to zero at SS. Secondly, the velocity starts from SS with a sharper increase than in the first stage and will extend to peak before returning to zero or near to zero at second SS. Thirdly, it starts from the second SS and after velocity reversals will touch a maximum value, twice rather than at case two, and go back down at a third SS. In the all these velocity cases, the velocity behaviours will make friction hysteretic loops, possibly because of increases in body velocity differing from decreases. The historical action of relative travels of wheel and body contributes to friction hysteresis.

In general, this friction model considers the static, stiction region and dynamic friction, which consists of the Stribeck effect, viscous friction and Coulomb friction. The mathematical model and summary for each part will be demonstrated in the next step.

7.1 Mathematical friction model

The mathematical expression for establishing the friction model gave the constituent terms described in order to accurately represent the observed phenomena, as shown in Eq. (12).

$$F_{\text{fric}} = \begin{cases} k_s(X_w - X_b) + b_d(\dot{X}_w - \dot{X}_b) \dot{X}_b = 0.0 \\ C_e e^{(|\dot{X}_b|/e1)} + \left[\frac{\mu(k_s(X_w - X_b) + b_d(\dot{X}_w - \dot{X}_b))}{\tan(\theta \mp \Delta\theta)} \right] + \sigma_v \dot{X}_b \dot{X}_b > 0.0 \\ -C_e e^{(|\dot{X}_b|/e1)} + \left[\frac{\mu(k_s(X_w - X_b) + b_d(\dot{X}_w - \dot{X}_b))}{\tan(\theta \mp \Delta\theta)} \right] + \sigma_v \dot{X}_b \dot{X}_b < 0.0 \end{cases} \quad (12)$$

Eq. (12) shows the friction model, which includes the two main parts of friction: static when, $\dot{X}_b = 0.0$, and dynamic, when $\dot{X}_b > 0.0$. The latter is presented by two expressions, depending on the velocity direction, and is discussed in detail later. In static friction, the stiction area is solely dependent on the velocity because the body velocity should be close to zero velocity or frequently just beyond zero velocity. The static model is accounted by the force balance of the test rig when the body was motionless, while the wheel was moved and describes the static friction sufficiently accurately. However, a dynamic model is necessary which introduces an extra state which can be regarded as transition and Coulomb and viscous friction. In addition to these friction models, steady physics state is also briefly discussed in this study.

7.2 Static friction model

After a test starts, the wheel begins to move respective to the road inputs, and initially the body remains motionless. This results from the static bearing friction and is undoubtedly a stick region body, $X_b = 0.0$. This friction component can be considered via the test rig vertical force balance $\sum F_v = 0.0$.

For the test rig, the following conventional model represents a 1/4-car without considering body friction as aforementioned by Eq. (1), the first reported implementation of friction forces within Newton's second law for a 1/4-car model [14], which leads to a new dynamic equation of motion for the mass body:

$$M_b \ddot{X}_b = [k_s(X_w - X_b) + b_d(\dot{X}_w - \dot{X}_b)] - F_{\text{fric}} \quad (13)$$

As described in the short period where the body remains motionless $X_b = 0.0$ and $\ddot{X}_b = 0.0$, Eq. (13) becomes

$$0.0 = [k_s(X_w - X_b) + b_d(\dot{X}_w - \dot{X}_b)] - F_{\text{fricS}} \quad (14)$$

then

$$F_{\text{fricS}} = [k_s(X_w - X_b) + b_d(\dot{X}_w - \dot{X}_b)] \quad (15)$$

where F_{fricS} is the static friction, which is a function of the relative displacements and relative velocities between the wheel and body multiplied by spring stiffness and viscous damper coefficients, with direction totally dependent on the next stage \dot{X}_b direction. This is considered as pre-sliding displacement, which exhibits how friction characteristics behave like a spring when the applied force is less than the static friction breakaway force. From the experimental work, amplitude input = 50 mm, it was found that the maximum stick friction force occasionally occurs at $(X_w - X_b) \leq 0.0069$ and $X_b \cong 0.0$.

7.3 Dynamic friction model

Earlier studies (see, e.g. [8, 10, 15]) have shown that a friction model involving dynamics is necessary to describe the friction phenomena accurately. A dynamic model describing the springlike behaviour during stiction was proposed by [16]. The Dahl model is essentially Coulomb friction with a lag in the change of friction force when the direction of motion is changed. The model has many commendable features and is theoretically well understood. Questions, such as the existence and uniqueness of solutions and hysteresis effects, were studied in an interesting paper by [17]. The Dahl model does not include the Stribeck effect. An attempt to incorporate this into the Dahl model was made by [18] where the authors introduced a second-order Dahl model using linear space-invariant descriptions. The Stribeck effect in this model is only transient; however, following a velocity reversal, it is not present in the steady-state friction characteristics. The Dahl model has been used for adaptive friction compensation [19, 20], with improved performance as a result. There are also other models for dynamic friction; Armstrong-Helouvry [8] proposed a seven-parameter model. This model does not combine the different friction phenomena but is, in fact, one model for stiction and another for sliding friction. Another dynamic model suggested by [21] had been used in connection with control by [15]. This model is not defined at zero velocity.

In this study, it was proposed that a nonlinear dynamic friction model combines the transition behaviour from stiction to the slide regime including the Stribeck effect, the Coulomb friction with consideration of the normal dynamic force at body bearings with suitable friction coefficient and the viscous friction dependent on the body velocity and appropriate viscous coefficient. This model involves arbitrary steady-state friction characteristics. The most crucial results of this model are to highlight precisely the hysteresis behaviours of friction relative to body velocity behaviour.

Referring to Eq. (12), there are two forms of dynamic friction, depending on the body velocity direction; it will be shown in detail as follows:

For $\dot{X}_b > 0.0$ the dynamic friction form is

$$F_{\text{fricD}} = \left\{ C_e e^{(|\dot{X}_b|/e1)} + \left[\frac{\mu(k_s(X_w - X_b) + b_d(\dot{X}_w - \dot{X}_b))}{\tan(\theta \mp \Delta\theta)} \right] + \sigma_v \dot{X}_b \right\} \quad (16)$$

From Eq. (16), it is clearly seen that dynamic friction consists of three parts. A summary is given for each: part one form is

$$F_{\text{fricT}} = C_e e^{(|\dot{X}_b|/e1)} \quad (17)$$

where F_{fricT} is transition friction, C_e is attracting parameter, $e1$ is the curvature degree and the absolute body velocity value meaning the direction of velocity is not affected. The transition friction has exponential behaviour with degrees identified experimentally and completely agrees with the literature review of most research studies regarding lubricant friction, which begins from the maximum value at the sticky region and quickly dips when the body just begins to move, or the body velocity is increased.

Secondly, F_{fricC} represents Coulomb friction, which is equal to the normal bearing force times the friction coefficient (μ), as follows:

$$F_{\text{fricC}} = \left\{ \frac{\mu(k_s(X_w - X_b) + b_d(\dot{X}_w - \dot{X}_b))}{\tan(\theta \mp \Delta\theta)} \right\} \quad (18)$$

where F_{fricC} is Coulomb friction with the opposite sign to velocity direction.

Finally, F_{fricV} represents viscous friction, which, because there is a lubricant contact between bearing and body, is counted by multiplying the body velocity with an appropriate viscous coefficient (σ_v).

$$F_{\text{fricV}} = \sigma_v \dot{X}_b \quad (19)$$

when $\dot{X}_b < 0.0$, the overall dynamic friction expression becomes

$$F_{\text{fricD}} = \left\{ -C_e e^{(|\dot{X}_b|/e1)} + \left[\frac{\mu(k_s(X_w - X_b) + b_d(\dot{X}_w - \dot{X}_b))}{\tan(\theta \mp \Delta\theta)} \right] + \sigma_v \dot{X}_b \right\} \quad (20)$$

Eq. (20) is similar to Eq. (16) as they have the same three terms but with a negative sign added in just for the transition friction term. This is because these values will describe the development friction in the opposite direction in the negative friction region.

The underlying motivation is that when the dynamic behaviour of the $1/4$ -car model is thoroughly understood, the knowledge can be used to design appropriate feedback controllers for active suspension systems with compensation for the friction forces.

7.4 Steady-state friction

It is vital to consider the friction behaviour within SS period. From **Figure 11** of body displacement as function of time, it is clear that the historical movement demeanour, which starts to move from the stiction region, $X_b = 0.0$ and $\dot{X}_b \cong 0.0$, is the first SS, stage (A), and then reaches the second SS, stage (B), at the mid-point of the road hydraulic actuator $X_b = 0.085$ m and $\dot{X}_b \cong 0.0$. Secondly, the body starts moving from the second SS and will reach the highest with a total amplitude $X_b = 0.135$ m and $\dot{X}_b \cong 0.0$ at the third SS, stage (C). Finally, it will start to move from the third SS stage and reach the lowest value of amplitude $X_b = 0.035$ m, travelling twice the distance compared with the second stage. Thus, it will finally achieve the four SS (D) at $X_b = 0.035$ m and $\dot{X}_b \cong 0.0$.

At body stiction and SS station, \ddot{X}_b is equal to zero. Therefore, the friction at steady state should be similar to static friction as mentioned in Section 7.2.

7.5 Simple friction model

Eq. (12) gives a general form for nonlinear friction occurring at the body supported lubricant bearings. This model could be studied from a different point of

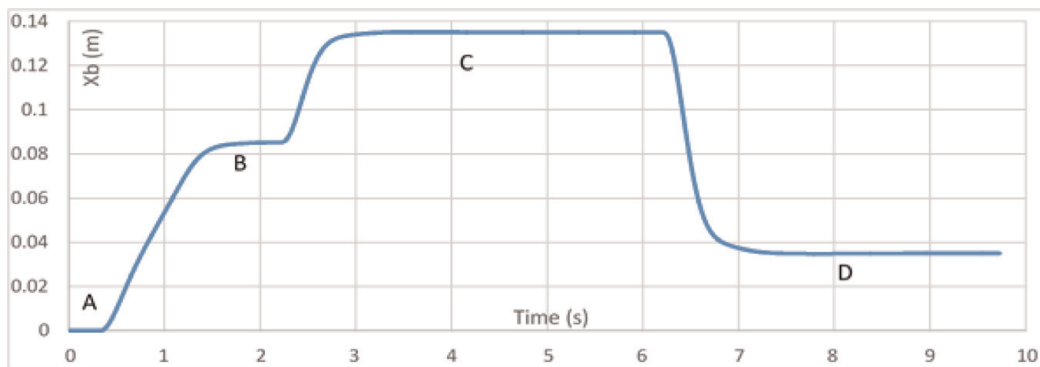


Figure 11.
Body displacement (X_b) with time.

view, whereby it can be returned to two dominant parameters, the body velocity and the normal body force, that could be termed damping friction relative to the body velocity and Coulomb friction qualified to normal body force.

For simplicity, even though the friction model, Eq. (12), reflected most of the observations measured using the system dynamics analysis and was used with the passive suspension model, it can still be employed in simple form through overlooking Coulomb friction. Therefore, the simple expression of friction without Coulomb friction is

$$F_{\text{fric}} = \begin{cases} k_s(X_w - X_b) + b_d(\dot{X}_w - \dot{X}_b)\dot{X}_b = 0.0 \\ C_e e^{(|\dot{X}_b|/e1)} + \sigma_v \dot{X}_b \dot{X}_b > 0.0 \\ -C_e e^{(|\dot{X}_b|/e1)} + \sigma_v \dot{X}_b \dot{X}_b < 0.0 \end{cases} \quad (21)$$

In Eq. (21), this model has the same three various forms dependent on \dot{X}_b , value and direction. Part one is the static friction, which has precisely the same shape for general friction, while the dynamic formula, damping friction, depending only on the body velocity in a different form by ignoring the Coulomb term. The interesting point is that, by implementing these simple friction forms, the simulation results also acquire a good agreement in comparison with the experimental results regarding system response parameters, which encouraged its use with the active suspension system. The question arises as to which one is more suitable for our case. Although the general friction model system, Eq. (12), gives more detail, depending on the system dynamics, and has the ability to highlight the hysteresis phenomenon that should occur with this system type, the simple friction model has lost this hysteresis.

However, the simple form also provides a real accord between the experimental and simulation results for system response, with little variation relative to that gained from considering general friction. From this point of view, a mathematical analysis is used, by using the residual mean square (RMS).

The RMS is defined as ‘a measure of the difference between data and a model of that data’. Therefore, two measured signals, X_b and $X_w - X_b$, will be used to show the accuracy of considering the general or simple friction forms.

RMS accounts for the measurement and simulation with and without Coulomb friction for relative movements between the wheel and body, as illustrated:

$$(RMS)_c = \sqrt{\frac{1}{N} \sum ((X_w - X_b)_m - (X_w - X_b)_{sc})^2} \quad (22)$$

and

$$(RMS) = \sqrt{\frac{1}{N} \sum ((X_w - X_b)_m - (X_w - X_b)_s)^2} \quad (23)$$

where $(RMS)_c$ and (RMS) are the RMS between the measured and simulation values with and without considering Coulomb friction, respectively, $(X_w - X_b)_m$ is the measured relative displacement, $(X_w - X_b)_{sc}$ and $(X_w - X_b)_s$ are the simulation data with and without implementing Coulomb friction and N is the total number of sample. The RMS results are shown in **Table 1**.

From **Table 1**, the RMS results show that using the friction model considering Coulomb friction is more accurate.

Signal	(RMS) _c	(RMS)
($X_w - X_b$)	0.006362	0.006366
X_b	0.096267	0.096386

Table 1.
RMS results.

8. Results

8.1 Friction results for general form (considering Coulomb friction)

Figure 12 shows friction force as a function of body velocity for the input force when amplitude = 50 mm, while the other cases when amplitude is = 30 or 70 mm. Accordingly, with the same friction behaviour, the same friction model can be used. It is apparent that the friction behaves as a hysteresis loop. Therefore, both sets of curves form a circle, enclosing a nonzero area, which is typical of dynamic friction besides the starting static friction. The loops enclosed three areas relating to velocity increases, decreases and directions. This is similar to expectations from the results of a dynamic friction model discussed in Sections 8.1 and 8.3. The upper portion of the curve shows the behaviour for increasing velocity when $\dot{X}_b > 0.0$ in two circumstances, while the lower portion shows the behaviour for decreasing velocity when $\dot{X}_b < 0.0$. This phenomenon may be a consequence of the dynamics of the process rather than of the nonlinearity; this phenomenon is often referred to as hysteresis. The hysteretic friction is, moreover, not a unique function of the velocity, but depends on the previous hysteresis of the movements.

In fact, there are two urgent situations that should be highlighted: the first is when the velocity equals zero, the body is motionless, and the friction values are similar to static friction values, as discussed in Section 7.2, while the second important situation is when the values of friction are within the SS situation, which has already been specified in the previous analysis in Section 7.4.

However, **Figure 12** shows the behaviour of friction relative to the body velocity. It is evident that the reaction in the stick region, or static friction at $X_b=0.0$, friction values start from zero and reach a maximum at the breakaway threshold force. From the experimental test, the breakaway force at the maximum relative displacement between X_w and X_b and the corresponding values for wheel and body velocity, accounted by Eq. (15), could be estimated. As a result, it was found to be equal to 193.8 N. Therefore, after the first positive position of static friction, because the direction of displacement moves up, whenever the body starts to move,

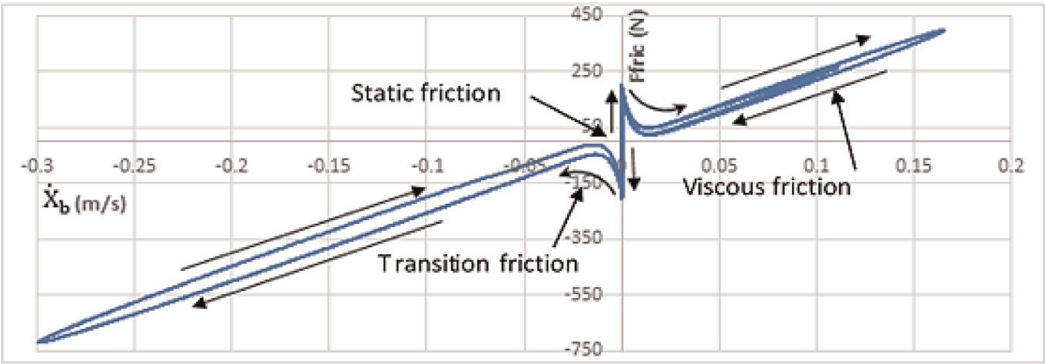


Figure 12.
Friction as function of the body velocity.

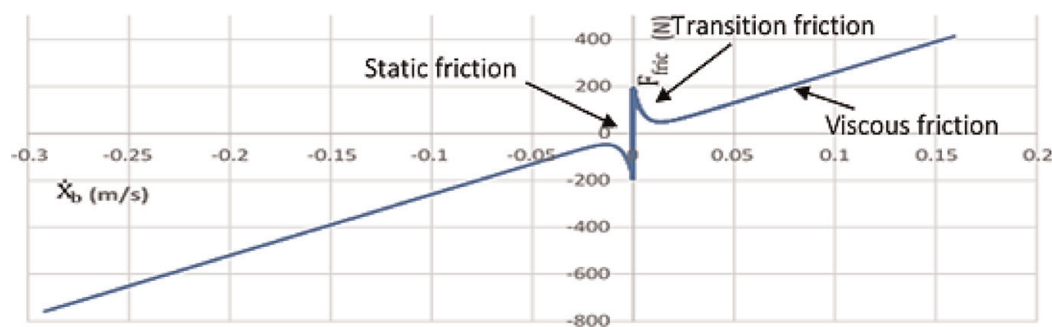


Figure 13.
Damping friction as a function of the body velocity.

when $\dot{X}_b > 0.0$, the friction hardly dips relative to the transition area from direct contact between body and bearings to mixed hydraulic contact. This clearly shows the Stribeck effects relative to hydraulic layer behaviour: a squeeze-film effect.

Following the system inputs and velocity value when $\dot{X}_b > 0.0$, the friction firstly draws a small, enclosed, positive cycle. After that, the body velocity returns to the second SS and increases to reach a maximum value before returning to the third SS with friction drawing a larger enclosed cycle in a positive direction. When $\dot{X}_b < 0.0$, the static values are equal to those for $\dot{X}_b > 0.0$ in the opposite direction, while the friction draws the most massive enclosed nonzero cycle with a value twice that of the larger enclosed cycle in the positive direction. This is because of the friction value and guidance following the road input and velocity values.

8.2 Friction results for simple form (without Coulomb friction)

In considering friction, while disregarding the Coulomb effects relative to the vertical force from the force inputs and the construction of the test rig, the inclination of the spring and damper from one side and the distance between the wheel unit and body mass from another side allows a promotion friction formula, damping friction, to be obtained. Although some features of friction characteristics, the hysteresis behaviour, will have been lost in considering this friction model with the passive suspension system design, success also has been achieved close to the experimental data. **Figure 13** shows the damping friction as a function of the body velocity when amplitude = 50 mm. It is approved that there is no hysteresis performance.

Meanwhile, **Figure 14** illustrates the association between damping and Coulomb friction. Although the damping friction is dominant, it remains vital to reflect the Coulomb friction in the general friction model, because it is responsible for bringing hysteresis performance to the model, and, as mentioned, this is quite essential to our system type.

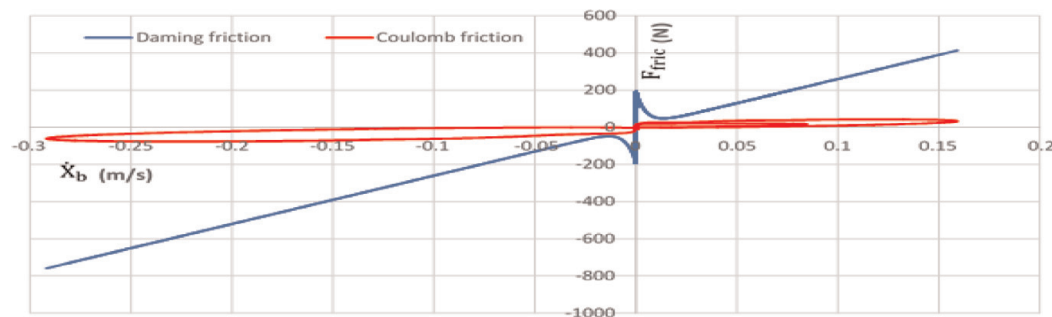


Figure 14.
Damping and Coulomb friction as a function of the body velocity.

9. Discussion

This chapter was set up to question the aspects of friction that merit inclusion with the $\frac{1}{4}$ car model. After a brief stating of the general frictional considerations, this discussion will review and summarise the findings.

Friction is a highly complex phenomenon, evolving at the contact of surfaces. Experiments demonstrate a functional addiction upon a significant change in parameters, including sliding speed, acceleration, critical sliding distance, normal load, surface preparation and material combination. In many engineering applications, the success of models in predicting experimental results remains strongly sensitive to the friction model. Friction is a natural phenomenon that is quite difficult to model and is not yet completely understood.

The investigation of the principal questions to inform the simulation framework were tested as follow: what is the most suitable technique for including friction in an analytical or numerical model, and what are the inferences of friction model superiority? The constituent elements are discussed in turn as follows:

9.1 The main reasons for considering friction

In this study, as shown in Section 3, considering and implementing the friction model within the equation of motion for the mass body is qualified for the following reasons:

1. Friction itself is crucial to find in any mechanical system. Friction exists everywhere, since degradation, precision, monitoring and control system are strongly affected by friction.
2. From the experiment test, it is clearly seen that there is no oscillation of mass body travels, while that was found with simulation model results. Therefore, a new term should be considered to overcome the issue, that is to say, a friction term.
3. In addition, from experimental measurements in Section 4.4, it is apparent that at the start of the test, while the wheel began to move in relation to road inputs, the body remained motionless for a period.

10. Conventional friction model

The majority of current model-based friction compensation schemes utilise classical friction models, such as Coulomb and viscous friction. In applications with high-precision positioning and with low-velocity following, the outcomes are not generally acceptable. Typical types are different combinations of Coulomb friction, viscous friction and the Stribeck effect, as has been mentioned in several researchers' works as shown in Section 5.

In this review, the established friction model, irrespective of its extreme effortlessness, can recreate all, that we are aware of, conditionally watched properties and features of low-velocity friction force dynamics. Considering the test rig schematic and the force information, there are three conditions, depending upon whether the body speed is speeding up or decelerating. Firstly, the velocity qualities start from zero, and soon after, velocity reversals reach the most elevated level and are maintained at zero, or close to zero, at SS. Secondly, the velocity begins from SS

with a sharper increment than in the first stage and will be stretched to the ultimate before it returns to zero, or near to zero, at SS. Thirdly, it will begin from SS and, after velocity reversals, will reach the highest estimate, twice the time as for case two, and spine to SS. In every one of these velocity cases, the velocity behaviour will make friction hysteretic loops that could account for the increments of body speed in a variety of paths from reductions.

In general, this friction model deliberates the static, stiction region and dynamic friction, which consists of the Stribeck effect, viscous friction and Coulomb friction, which rely on the dynamic tangential force, which evolves in the test rig contact bearings. Therefore, there are general and simple friction forms as follows:

10.1 Mathematical friction model

$$F_{\text{fric}} = \begin{cases} k_s(X_w - X_b) + b_d(\dot{X}_w - \dot{X}_b) \dot{X}_b = 0.0 \\ C_e e^{(|\dot{X}_b|/e1)} + \left[\frac{\mu(k_s(X_w - X_b) + b_d(\dot{X}_w - \dot{X}_b))}{\tan(\theta \mp \Delta\theta)} \right] + \sigma_v \dot{X}_b \dot{X}_b > 0.0 \\ -C_e e^{(|\dot{X}_b|/e1)} + \left[\frac{\mu(k_s(X_w - X_b) + b_d(\dot{X}_w - \dot{X}_b))}{\tan(\theta \mp \Delta\theta)} \right] + \sigma_v \dot{X}_b \dot{X}_b < 0.0 \end{cases} \quad (24)$$

This mathematical eq. (24) incorporates two primary parts of friction: static and dynamic friction. The latter as two expressions and is influenced by the velocity track. In static friction, the stiction area is exclusively not subject to the velocity because the body velocity should be close to zero velocity or just beyond zero velocity. Frequently, the static models are numbered by the strength adjustment of the test rig when the body sticks, while the wheel is moved and depicts the static friction sufficiently precisely. A dynamic model is vital to present an additional state, which can be viewed as the transition, Coulomb and viscous friction. In addition to these friction models, steady physics state is also briefly discussed in this study.

10.2 Simple friction model

When be ignored the Coulomb friction, the previous nonlinear friction model shown in Eq. (12) becomes a simple model, as illustrated in Eq. (21), despite losing some features of friction characteristics with this model, in comparison with experimental data that also obtained close results. From this aspect, another approach should be found to discover which approach obtains more accurate results by comparing with measured results. By using RMS mathematical analysis, the results shown in **Table 1** prove, as an outcome, that the friction model is more accurate with a consideration of Coulomb friction.

11. Conclusion

An accurate nonlinear dynamic model for friction has been presented. The model is simple yet captures most friction phenomena that are of interest for simulated test results. The low-velocity friction characteristics are particularly

important for high-performance pointing and tracking. The model can describe arbitrary steady-state friction characteristics. It supports hysteretic behaviour due to frictional lag and springlike behaviour in stiction and gives a different breakaway force depending on the rate of change of the applied force. All these phenomena are unified into static, steady-state and dynamic friction equations. The model can be readily used in simulations of systems with friction.

It is essential to consider friction in this study, in the hope that the study creates an opening and contributes towards a reconsideration of the role of friction using the current quarter in half- and full-car suspension models.

Simulation leads to the same conclusion as proven by the experimental results obtained from the test rig test. Comparison between experimental and simulation results show that the proposed general friction model is more accurate than the conventional models (simple model).

Acknowledgements


I highly appreciate my original university, Kerbala University, and Cardiff University for giving me a chance to do this work. At the same time, I thank the technician people in the laboratory for helping.

Author details

Ali I. H. Al-Zughaibi
Engineering College, Kerbala University, Karbala, Iraq

*Address all correspondence to: ali.i@uokerbala.edu.iq

IntechOpen

© 2019 The Author(s). Licensee IntechOpen. This chapter is distributed under the terms of the Creative Commons Attribution License (<http://creativecommons.org/licenses/by/3.0>), which permits unrestricted use, distribution, and reproduction in any medium, provided the original work is properly cited. 

References

- [1] Nichols S. MANE 6960 Friction & Wear of Materials; 2007
- [2] Al-Bender F et al. A novel generic model at asperity level for dry friction force dynamics. *Tribology Letters*. 2004;**16**(1):81-93. DOI: 10.1023/B:TRIL.0000009718.60501.74
- [3] De Wit CC et al. A new model for control of systems with friction. *IEEE Transactions on Automatic Control*. 1995;**40**(3):419-425. DOI: 10.1109/9.376053
- [4] Rabinowicz E. Friction and wear of materials. *Journal of Applied Mechanics*. 1965;**33**(1966):479. DOI: 10.1115/1.3625110
- [5] Al-Zughaibi AIH. Experimental and analytical investigations of friction at lubricant bearings in passive suspension systems. *An International Journal of Nonlinear Dynamics and Chaos in Engineering Systems*. 2018;**94**(2): 1227-1242. DOI: 10.1007/s11071-018-4420-x (Open Access)
- [6] Surawattanawan P. The influence of hydraulic system dynamics on the behaviour of a vehicle active suspension [thesis]. Cardiff, UK: Cardiff University; 2000
- [7] Watton J. Chapter 3: Modelling, Monitoring and Diagnostic Techniques for Fluid Power Systems. London: Springer Science & Business Media; 2005. pp. 182-186. ISBN-13: 9781846283734
- [8] Armstrong-Helouvry B. Control of Machines with Friction. Vol. 128. New York: Springer Science & Business Media; 2012
- [9] Lischinsky P et al. Friction compensation for an industrial hydraulic robot. *IEEE Control Systems Magazine*. 1999;**19**(1):25-32. DOI: 10.1109/37.745763
- [10] Armstrong-Hélouvry B et al. A survey of models, analysis tools and compensation methods for the control of machines with friction. *Automatica*. 1994;**30**(7):1083-1138. DOI: 10.1016/0005-1098(94)90209-7
- [11] Tsurata K et al., editors. Genetic algorithm (GA) based modelling of nonlinear behaviour of friction of a rolling ball guide way. In: *Proceedings 6th International Workshop on Advanced Motion Control*; 30 March-1 April 2000. Nagoya, Japan: IEEE; 2002
- [12] Smyth AW et al. Development of adaptive modelling techniques for non-linear hysteretic systems. *International Journal of Non-Linear Mechanics*. 2002; **37**(8):1435-1451. DOI: 10.1016/S0020-7462(02)00031-8
- [13] Altpeter F. Friction modelling, identification and compensation. *École Polytechnique Fédérale de Lausanne*; 1999. DOI: 10.5075/epfl-thesis-1988
- [14] Al-Zughaibi A et al. A new insight into modelling passive suspension real test rig system, quarter race car, with considering nonlinear friction forces; ImechE, part D. *Journal of Automobile Engineering*. 2018;**233**(8):2257-2266. DOI: 10.1177/0954407018764942
- [15] Dupont PE. Avoiding stick-slip through PD control. *IEEE Transactions on Automatic Control*. 1994;**39**(5): 1094-1097. DOI: 10.1109/9.284901
- [16] Dahl PR. A solid friction Model. No. TOR-0158 (3107-18)-1. Segundo, CA: Aerospace Corp El; 1968
- [17] Bliman P-A. Mathematical study of the Dahl's friction model. *European Journal of Mechanics. A, Solids*. 1992; **11**(6):835-848 ISSN: 0997-7538

[18] Bliman P, Sorine M. Friction modelling by hysteresis operators. Application to Dahl, stiction and Stribeck effects. In: Proc. Conf. on Models of Hysteresis; Trento. 1991. p. 10

[19] Walrath CD. Adaptive bearing friction compensation based on recent knowledge of dynamic friction. *Automatica*. 1984;**20**(6):717-727. DOI: 10.1016/0005-1098(84)90081-5

[20] Leonard NE, Krishnaprasad PS, editors. Adaptive friction compensation for bi-directional low-velocity position tracking. In: Proceedings of the 31st IEEE Conference on Decision and Control; 16-18 December 1992. Tucson, AZ, USA: IEEE; 2002

[21] Ruina A, Rice J. Stability of steady frictional slipping. *Journal of Applied Mechanics*. 1983;**50**(2):343-349. DOI: 10.1115/1.3167042